



OPEN

SUBJECT AREAS:
PHYLOGENETICS
TAXONOMYReceived
22 November 2013Accepted
21 March 2014Published
10 April 2014Correspondence and
requests for materials
should be addressed to
A.Y. (yabukia@
jamstec.go.jp)* These authors
contributed equally to
this work.† Current address:
Canadian Institute for
Advanced Research,
Department of Botany,
University of British
Columbia, Vancouver,
British Columbia,
Canada.‡ Current address:
National Research
Institute of Fisheries
Science, Fisheries
Research Agency,
Yokohama,
Kanagawa, Japan.

Palpitomonas bilix represents a basal cryptist lineage: insight into the character evolution in Cryptista

Akinori Yabuki^{1*}, Ryoma Kamikawa^{2,3*}, Sohta A. Ishikawa^{4,5}, Martin Kolisko^{6†}, Eunsoo Kim⁷, Akifumi S. Tanabe^{4‡}, Keitaro Kume⁵, Ken-ichiro Ishida⁵ & Yuji Inagaki^{5,8}

¹Japan Agency for Marine-Earth Science and Technology (JAMSTEC), Yokosuka, Kanagawa, Japan, ²Graduate School of Human and Environmental Studies, Kyoto University, Kyoto, Kyoto, Japan, ³Graduate School of Global Environmental Studies, Kyoto University, Kyoto, Kyoto, Japan, ⁴Graduate School of Life and Environmental Sciences, University of Tsukuba, Tsukuba, Ibaraki, Japan, ⁵Graduate School of Systems and Information Engineering, University of Tsukuba, Tsukuba, Ibaraki, Japan, ⁶Departments of Biology, Dalhousie University, Halifax, Nova Scotia, Canada, ⁷Sackler Institute for Comparative Genomics and Division of Invertebrate Zoology, American Museum of Natural History, New York, NY, USA, ⁸Center for Computational Sciences, University of Tsukuba, Tsukuba, Ibaraki, Japan.

Phylogenetic position of the marine biflagellate *Palpitomonas bilix* is intriguing, since several ultrastructural characteristics implied its evolutionary connection to Archaeplastida or Hacrobia. The origin and early evolution of these two eukaryotic assemblages have yet to be fully elucidated, and *P. bilix* may be a key lineage in tracing those groups' early evolution. In the present study, we analyzed a 'phylogenomic' alignment of 157 genes to clarify the position of *P. bilix* in eukaryotic phylogeny. In the 157-gene phylogeny, *P. bilix* was found to be basal to a clade of cryptophytes, goniomonads and kathablepharids, collectively known as Cryptista, which is proposed to be a part of the larger taxonomic assemblage Hacrobia. We here discuss the taxonomic assignment of *P. bilix*, and character evolution in Cryptista.

Resolving the phylogenetic relationship amongst major eukaryotic lineages is one of the most challenging subjects in evolutionary biology. In theory, the full diversity of eukaryotes needs to be grasped prior to reconstructing global eukaryotic phylogeny. However, our current knowledge regarding microbial eukaryotes, which comprise the main body of eukaryotic diversity, is insufficient (e.g.^{1,2}). Traditionally, our knowledge of the diversity of microbial eukaryotes has been expanded by isolating and cultivating novel organisms—some of these, like for example *Chromera velia*³ and *Rigifila ramosa*⁴, have been indeed significant for improving our understanding of the origin and evolution of eukaryotes. Once the culture strains are established, we can collect physiological, ultrastructural, and molecular data from the cells of interest. However, currently uncultivable microbial eukaryotes are not possible to study in detail by this culture-dependent approach. A recent culture-independent approach, which assesses nucleotide sequence data extracted from eukaryotes in an environmental sample, provides great opportunities for shedding light on the phylogenetically diverse uncultured microbial eukaryotes (e.g.^{1,2}). This approach became one of the standard techniques to survey biodiversity; however, it cannot offer comprehensive knowledge on the individual organism associated with a particular environmental sequence. Practically, neither culture-independent nor culture-dependent approach is dispensable to study biodiversity and organismal phylogeny of eukaryotes. Indeed, the combination of the two approaches successfully established the connection between *Picomonas judraskeda* and '(pico)biliphytes', which were recognized initially by small subunit ribosomal RNA sequences amplified from the seawater samples^{5,6}.

Palpitomonas bilix is a marine heterotrophic biflagellate with uncertain taxonomic affiliation⁷; a phylogenetic analysis of six nuclear genes failed to settle the position of *P. bilix* in global eukaryotic phylogeny. The combination of the morphological and ultrastructural characteristics of *P. bilix* was novel, albeit some ultrastructural characteristics of this flagellate hinted its possible affinity to the Archaeplastida or Hacrobia. Archaeplastida is composed of three lineages (i.e., green plants, rhodophytes and glaucophytes); these groups are believed to be the direct descendants of the first plastid-bearing eukaryote⁸. Nevertheless it remains uncertain how the cyanobacterial endosymbiosis transformed a heterotrophic eukaryote into the common ancestor of Archaeplastida, since no clear phylogenetic affinity has been recovered between Archaeplastida and any of the extant heterotrophic



lineages. If *P. bilix* is truly related to Archaeplastida, this heterotrophic flagellate likely holds keys to understanding the early evolution of plastids. In contrast to Archaeplastida, Hacrobia is a diverse group comprising both phototrophs (i.e., cryptophytes and haptophytes) and heterotrophs^{9,10}. The plastid genomes of cryptophytes and haptophytes were found to encode a ribosomal protein gene (*rpl36*) laterally acquired from a bacterium, suggesting that the two photosynthetic lineages were derived from a single photosynthetic ancestor, of which plastid genome encoded the laterally transferred *rpl36*¹¹. On the other hand, it is widely accepted that cryptophytes possess apparent closer evolutionary affinities to heterotrophic lineages (i.e. goniomonads and kathablepharids), than they are to haptophytes, in the tree of eukaryotes^{7,12}, indicating that cryptophytes and haptophytes are seemingly separated by multiple heterotrophic lineages. Thus, two competing scenarios are possible to explain how cryptophytes and haptophytes share the plastids with the *rpl36* of bacterial origin^{13,14}. If the most recent ancestor of cryptophytes and haptophytes (i.e. ancestral hacrobian cell) was phototrophic, all the descendants, except cryptophytes and haptophytes, secondarily lost the original plastid. The alternative scenario, which assumes the ancestral hacrobian cell as heterotrophic, demands two separate plastid acquisitions, one on the branch leading to cryptophytes and the other on the branch leading to haptophytes. Furthermore, a recent phylogenetic study by Burki et al.¹⁵ casted doubt on the monophyly of Hacrobia, albeit *P. bilix* was absent in their analyses. Thus, elucidating the precise position of *P. bilix* may be significant to further evaluate the validity of Hacrobia monophyly, and the plastid evolution of the descendants of the last common ancestor of cryptophytes and/or haptophytes.

We here conducted transcriptomic analyses of *P. bilix* and the cryptomonad *Goniomonas* sp., and assembled an alignment composed of 157 genes. Our ‘phylogenomic’ analysis of the 157-gene alignment successfully clarified the phylogenetic position of *P. bilix* in global eukaryotic phylogeny: *P. bilix* branched at the base of the assemblage of Cryptophyceae (cryptophytes), Goniomonadea (goniomonads), and Leucocrypta (kathablepharids) that are the members of phylum Cryptista¹⁰ with high statistical support. In light of the phylogenetic relationship among *P. bilix*, cryptophytes, goniomonads, and kathablepharids, the character evolution of this monophyletic assemblage is discussed.

Results

Genomic and/or transcriptomic data from 64 eukaryotes were assembled into a 157-gene alignment containing 41,372 unambiguously aligned amino acid positions. Note that we excluded sequence data of uncultivated cells from environmental samples, which were potentially contaminated with distantly related organisms, from this alignment. In the maximum-likelihood (ML) analysis of the 157-gene alignment, we recovered a well-supported clade of stramenopiles, alveolates, and rhizarians (SAR¹⁶); and one of *Tsukubamonas globosa*, jakobids, euglenozoans, and heteroloboseans (Discoba¹⁷), all of which were resolved in pioneering phylogenomic analyses (Fig. 1). Monophyly of neither Excavata nor Hacrobia was positively favored in the ML analyses of the 157-gene alignment, consistent with other phylogenomic studies (e.g.^{15,18}). The tree topology from Bayesian analysis was fundamentally congruent with that from the ML analysis, except for two points: (i) monophyly of Archaeplastida was recovered with a Bayesian posterior probability (BPP) of 1.00 and (ii) the centrohelid *Polyplacocystis contractilis* (previously known as *Raphidiophrys contractilis*) grouped with haptophytes with a BPP of 0.96 (data not shown). As anticipated from phylogenies of small subunit rRNA (SSU rRNA) sequences (e.g.¹²), our phylogenomic analyses united cryptophytes and *Goniomonas* sp., with a ML bootstrap percentage value (MLBP) of 100% and a BPP of 1.00 (Fig. 1). The clade of cryptophytes and *Goniomonas* sp. was then connected to the kathablepharid *Roombia truncata* with a MLBP of 95% and a

BPP of 1.00, which is in good agreement with the results presented in Burki et al.¹⁵ and SSU rRNA phylogenies (e.g.¹²). Finally, *P. bilix* branched at the base of the clade of cryptophytes, *Goniomonas* sp., and *R. truncata* with a MLBP of 91% and a BPP of 1.00 (Fig. 1). We additionally conducted the ML analysis including the genomic data amplified from an uncultured picozoan cell¹⁹ (Fig. S1). However, the picozoan sequences showed no specific affinity to any members of Cryptista (including *P. bilix*) or groups/species considered in our dataset (Fig. S1).

The roll-shaped ejective organelle, i.e., ejectosome (occasionally called as ‘trichocysts’), is identified in cryptomonads, kathablepharids and a few prasinophytes²⁰. Major proteins, which comprise cylindrical coiled ribbons in the ejectosomes of the cryptophyte *Pyrenomonas helgolandii*, were found to be encoded by *tri1*, *tri2*, *tri3-1*, and *tri3-2*²¹. We here surveyed *tri* genes/transcripts in the complete genome of the cryptophyte *Guillardia theta*, and transcriptomic data from the goniomonad *Goniomonas* sp. and the kathablepharid *R. truncata* (PRJNA73793¹⁵). The *Gu. theta* genome was found to possess four *tri1*, eight *tri2/3-1*, and four *tri3-2* genes (Fig. 2; Note that *tri2* and *tri3-1* are not distinguishable at the amino acid sequence level). We found four *tri2/3-1* and three *tri3-2* sequences in the transcriptomic data from *Goniomonas* sp. Two *tri2/3-1* and one of *tri3-2* sequences were additionally detected from the transcriptome data of another goniomonad species (*Goniomonas avonlea*; these data were recently generated as a part of the Marine Microbial Eukaryote Transcriptome Sequencing Project funded by the National Center for Genome Resources and the Gordon and Betty Moore Foundation’s Marine Microbiology Initiative: <http://marinemicroeukaryotes.org/>). Likewise, the transcriptomic data from *R. truncata* contained three *tri2/3-1* and two *tri3-2* sequences. No *tri1* sequence was detected in the data from *Goniomonas* sp., *Go. avonlea* or *R. truncata* even by a sensitive amino acid sequence similarity search using probabilistic methods (HMMER²²; data not shown).

While the 157-gene phylogeny strongly suggests the close affinity of *P. bilix* to the cryptomonad-kathablepharid clade (Fig. 1), ejectosomes or ejectosome-like structures were not reported from *P. bilix*⁷. Consistent with the absence of ejectosomes at the level of ultrastructural observation, we failed to identify any types of *tri* sequences in the transcriptomic data from *P. bilix*.

Discussion

We successfully resolved the phylogenetic position of *P. bilix* by analyzing the 157-gene alignment. This ‘orphan’ flagellate was found to form a robust clade with cryptomonads (i.e., cryptophytes and goniomonads) and the kathablepharid *R. truncata*. The result presented here supports a taxonomic assignment by Cavalier-Smith^{10,23}, in which *P. bilix* was placed into subphylum Palpitia under phylum Cryptista. In the 157-gene phylogeny, *P. bilix* was recovered as the earliest branching lineage amongst cryptists with high statistical support. Cryptomonads have been observed to form a clade with kathablepharids, rather than *P. bilix*, in phylogenetic analyses of SSU rRNA sequences in which all of *P. bilix*, cryptomonads and kathablepharids were considered (e.g.^{7,12}). Likewise, the ML analysis of a small-scale multigene alignment united cryptomonads with the kathablepharid *Leucocryptos marina*, not with *P. bilix*⁷. As the relationship among *P. bilix*, cryptomonads and kathablepharids inferred from the present phylogenomic analyses and SSU rRNA/small-scale multigene phylogenies are consistent with one another, we conclude that cryptomonads are more closely related to kathablepharids than they are to *P. bilix* within the Cryptista clade.

An earlier study suggested that Picozoa may be related to cryptomonads⁶. To further examine the possible close relationship between Picozoa and Cryptista including *P. bilix*, we subjected a phylogenomic alignment including the genomic data, which were generated from a single picozoan cell isolated from seawater¹⁹, to the ML analysis. Unfortunately, the additional ML analysis was not able to

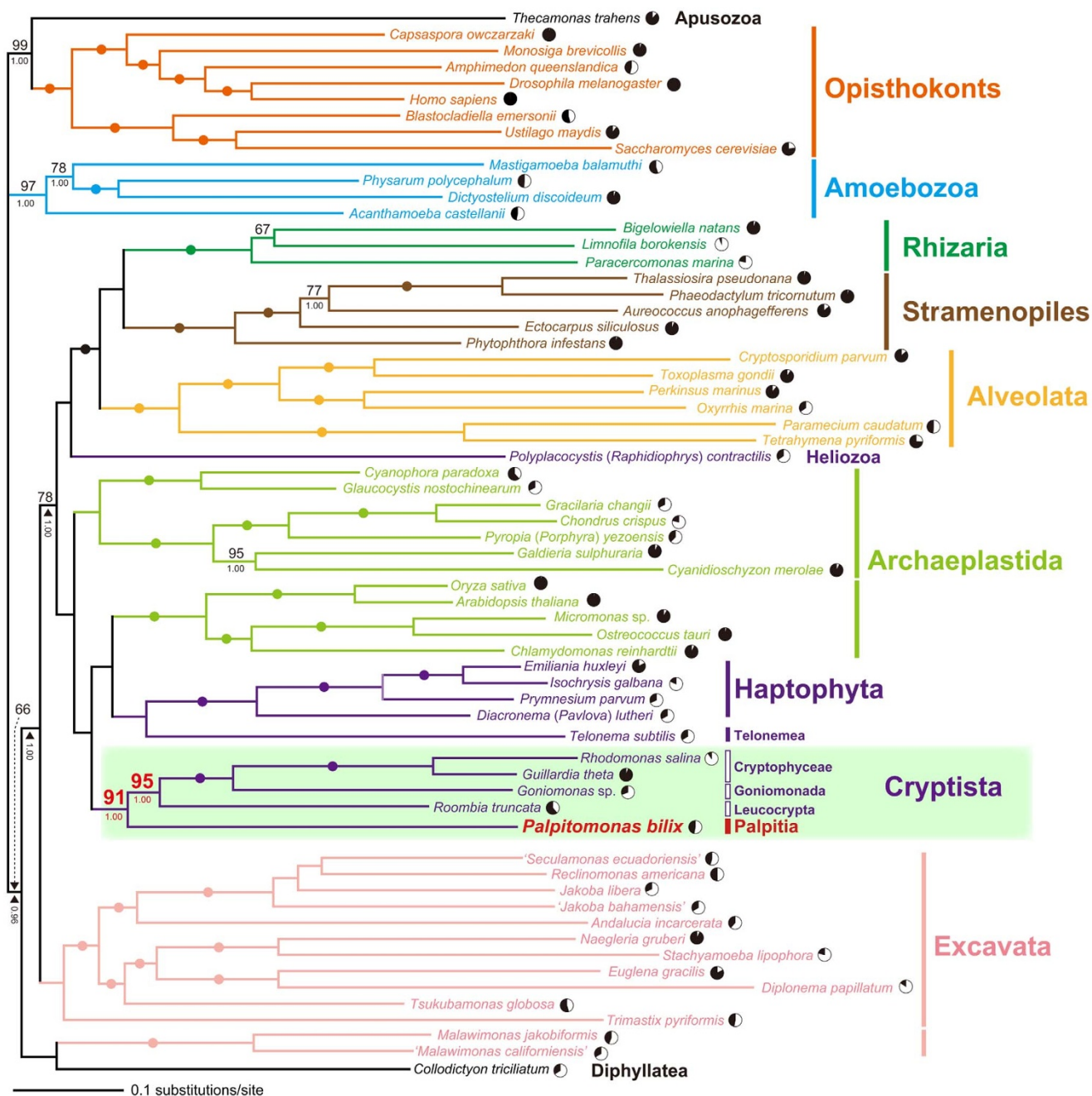


Figure 1 | Phylogenetic position of *Palpitomonas bilix* inferred from the maximum-likelihood (ML) analysis of a 157-gene alignment (41,372 amino acid positions). The 157-protein alignment was analyzed by both maximum-likelihood (ML) and Bayesian methods. As the two methods reconstructed very similar trees, only the ML tree is shown here. Upper and lower values at nodes represent ML bootstrap percentage values (MLBPs) and Bayesian posterior probabilities (BPPs). MLBPs <60% and BPPs <0.95 are omitted from the figure. Dots correspond to MLBP of 100% and BPP of 1.00.

resolve the precise position of the picozoan sequences in the tree of eukaryotes (Fig. S1), being consistent with the previous phylogenomic studies¹⁵. As a large portion (86%) of the picozoan sequences in our phylogenomic alignment is missing, the position of Picozoa needs to be revisited after future genomic and/or transcriptomic analyses on a cultured picozoan strain.

The reliable relationship among *P. bilix*, cryptomonads and kathablepharids enables us to propose evolutionary scenarios for some morphological and ultrastructural characteristics shared amongst cryptists (see below). *Palpitomonas bilix* and cryptomonads possess flat mitochondrial cristae^{7,24,25}, while kathablepharids have tubular cristae²⁶. Thus, we propose that flat mitochondrial crista is an ancestral characteristic of cryptists (see 'LCAC' in Fig. 3a), and a 'flat-to-

tubular' transformation of mitochondrial cristae occurred on the branch leading to kathablepharids (marked 'A' in Fig. 3a). However, we cannot exclude the alternative possibility, which assumes that the LCAC possessed tubular cristae, and 'tubular-to-flat' transformation of mitochondrial cristae occurred on the multiple branches in the Cryptista clade.

The ornamental structures of the cell membrane vary among cryptist members. While *P. bilix* is a naked cell without any obvious ornamental structures, the cell membrane of cryptomonads is sandwiched by proteinaceous plates called periplasts²⁴ and that of kathablepharids is covered by a sheath structure²⁶. The sheath structure of kathablepharids is composed of structurally distinct two layers²⁷ and seems to be distinct from the periplast of cryptomonads in origin.



(a) Tri2/3-1

<i>Pyrenomonas helgolandii</i> Tri2 (JF826282)	-----MRTVLYGKKAANLYTQAFVQNTQARALYQESEDITYYRANDAASDDWRRRARHQWDYFYNRH--
<i>Guillardia theta</i> (154813)	-----MRTILYGKKAANLYTQAFVQNTQARALYQESEDITYYRANDAASDDWRRRARHQWDYFYNRH--
<i>Guillardia theta</i> (153070)	-----MTEELYGKHAALYAQAADFNTARFYVMKQADAYLANAQAASDDWRRRARHQWDYFYRRK--
<i>Guillardia theta</i> (154049)	-----MTEQLYGKHAALYAQAADFNTARFYVMKQADAYLANAQAASDDWRRRARHQWDYFYRRK--
<i>Roombia truncata</i> (JP440959)	--MGFIKTKLYGKSTAAALYQAAADFNTARFYVMKQADAYLANAQAASDDWRRRARHQWDYFYHRS--
<i>Guillardia theta</i> (149850)	-----MRTILYGKKAANLYTQAGDYQKTARFYVMKQADAYLANAQAASDDWRRRARHQWDYFYHRS--
<i>Guillardia theta</i> (156612)	-----MFETLYGKKAANLYTQAGDYQKTARFYVMKQADAYLANAQAASDDWRRRARHQWDYFYHRS--
<i>Guillardia theta</i> (150127)	-----MFQALYGKKAANLYTQAGDYQKTARFYVMKQADAYLANAQAASDDWRRRARHQWDYFYHRS--
<i>Goniomonas</i> sp. (c248)	-----MFCELYGKKAANLYTQAGDYQKTARFYVMKQADAYLANAQAASDDWRRRARHQWDYFYHRS--
<i>Goniomonas avonlea</i> (66650)	-----MVFSELYGKKAANLYTQAGDYQKTARFYVMKQADAYLANAQAASDDWRRRARHQWDYFYHRS--
<i>R. truncata</i> (JP448631)	GKFAANIQTLYGPTAAAMYEKAAASLNKQARSTYEESEANAYFQANSAAADDMKRRARHQWDYFYHRS--
<i>Goniomonas</i> sp. (67305)	-----MVKTLQLYGSLAAGMYSKGFQANLAARKLWQKSEDTYQANDAASDDWRRRARHQWDYFYHRS--
<i>Goniomonas avonlea</i> (c845)	-----MQVQLYGSLAAGMYSKGFQANLAARKLWQKSEDTYQANDAASDDWRRRARHQWDYFYHRS--
<i>R. truncata</i> (JP44873)	-----MFQLLYGSLAAGL YDQAALNANARVLYLKSSDTYKANDAASDDWRRRARHQWDYFYHRS--
<i>Guillardia theta</i> (153735)	-----MFSVLYGQTAALYAKAAGQNAQARQLYNASADTYKANDAASDDWRRRARHQWDYFYHRS--
<i>Guillardia theta</i> (156313)	-----MFQTLYGGTAALYAKAAGQNAQARQLYNASADTYKANDAASDDWRRRARHQWDYFYHRS--
<i>Goniomonas</i> sp. (c2090)	-----MFQLLYGQTAAGLYAAAAGQNAKARQLYNASADTYKANDAASDDWRRRARHQWDYFYHRS--
<i>Goniomonas</i> sp. (c1105)	-----MFQLLYGKTAAGLYAAAAGQNAKARQLYNASADTYKANDAASDDWRRRARHQWDYFYHRS--
<i>P. helgolandii</i> Tri3-1 (JF710318)	-----MFQTLYGGTAALYAKAAGQNAQARQLYNASADTYKANDAASDDWRRRARHQWDYFYHRS--

(b) Tri3-2

<i>P. helgolandii</i> Tri3-1 (JF710319)	MIAKLFDFLEDYAGTYRETRNAYLKAANQLKLLATGPYKARDAYVAATATYTKSLYE
<i>Guillardia theta</i> (153651)	MIQKLFDFLEDYAGTYRETRNAYLKAANQLKLLATGPYKARDAYVAATATYTKSLYE
<i>Goniomonas</i> sp. (c32651)	MLAKLFDFLEDYAGTYRETRNAYLKAANQLKLLATGPYKARDAYVAATATYTKSLYE
<i>Goniomonas avonlea</i> (58518)	MFALLDFLEDYAGTYRATRDAYLKAANQLKLLATGP-----
<i>Guillardia theta</i> (154597)	MFALLDFLEDYATYRATRDAYLKAANQLKLLATGPYKARDAYVAATATYTKSLYE
<i>Guillardia theta</i> (155364)	MFSLLDFLEDYATYRATRDAYLKAANQLKLLATGPYKARDAYVAATATYTKSLYE
<i>Goniomonas</i> sp. (c7284)	MFALLDFLEDYAGTYRATRDAYLKAANQLKLLATGPYKARDAYVAATATYTKSLYE
<i>Goniomonas</i> sp. (c608)	MFALLDFLEDYAGTYRATRDAYLKAANQLKLLATGPYKARDAYVAATATYTKSLYE
<i>R. truncata</i> (JP448944)	MFTQLDFLEDYAGTYRATRDAYLKAANQLKLLATGPYKARDAYVAATATYTKGLYE
<i>Guillardia theta</i> (153377)	MFQLLFDLGDYATYRATRDAYLKAANQLKLLATGPYKARDAYVAGTATYTKGLYE
<i>R. truncata</i> (JP448954)	MFQLLDFLEDYAKTYRETRDDYLKAANALKLLATGPYKARDAYVAGTATYTKGLYE

Figure 2 | Putative protein components of the ejectisomes. (a). Tri2/3-1 amino acid sequence alignment. Note that Tri2 and Tri3-1 are indistinguishable based on sequence analyses. Amino acid residues shared among more than 15 out of the 19 homologues are shaded. GenBank accession numbers for the amino acid sequences *Pyrenomonas helgolandii* Tri2 and Tri3-1 are shown in parentheses. For Tri2/3-1 homologues of *Guillardia theta*, the protein ids are shown in parentheses. For those of *R. truncata* and those of *Goniomonas* sp. and *Go. avonlea*, the Genbank accession numbers and contig numbers of their corresponding nucleotide sequences are shown in parentheses, respectively. (b). Tri3-2 amino acid sequence alignment. Amino acid residues shared among more than 9 out of the 11 homologues are shaded. The numbers in parentheses are shown with the same manner as adopted in Figure 2a.

Consequently, it may be reasonable to consider that they are not homologous structures. We here propose that the ancestral cryptist possessed no ornamental elaboration of the cell membrane (see 'LCAC' in Fig. 3a), and the sheath structure and periplast emerged on the branches leading to kathablepharids and cryptomonads, respectively (marked 'A' and 'B' in Fig. 3a).

Ultrastructurally characterized species of kathablepharids such as *Kathablepharis* spp. possess a conoid-shaped feeding apparatus, which resembles superficially the apical complex of apicomplexan parasites²⁶. As no conoid-shaped feeding apparatus has been found in any cryptists except kathablepharids, this structure was likely invented on the branch leading to kathablepharids (marked 'A' in Fig. 3a) and enabled the flagellates to feed on large-sized prey cells, such as eukaryotic algae (note that goniomonads and *P. bilix* are bacteriovorous).

Variation in flagellar appendages has been reported among cryptist members. Bipartite flagellar hairs were reported in both *P. bilix* and cryptophytes^{7,28}. The flagellum of goniomonads has spines and simple flagellar hairs²⁸. The sheath structures that cover the surfaces of kathablepharid cells are further extended to the flagella. Thus, the variation in flagellar accessories found in the Cryptista clade can be reconciled as follows; the ancestral cryptist possessed flagella with bipartite hairs, and this feature has been retained in cryptophytes and *P. bilix* (see 'LCAC' in Fig. 3a). It remains unclear whether the ancestral flagella were equipped with a 'cryptophyte-like' bilateral row or '*P. bilix*-like' unilateral row of bipartite hairs. After the divergence of major cryptist lineages, the bipartite flagellar hairs were likely substituted by the spines/simple hairs on the branch leading to goniomonads (marked 'C' in Fig. 3a), and replaced by the sheath structures on the branch leading to kathablepharids (marked 'A' in Fig. 3a).

Unlike the characteristics discussed above, we can investigate the evolution of the ejectisomes in Cryptista at both ultrastructural and

molecular levels. Ejectisomes are found in cryptomonads and kathablepharids²⁰, but not in *P. bilix*⁷. As *P. bilix* is basal to ejectisome-bearing members of Cryptista, this ejective organelle was most likely established in the common ancestor of cryptomonads and kathablepharids (marked 'D' in Fig. 3a). We found *tri* gene transcripts in the transcriptomic data from all of the ejectisome-bearing cryptist members. In contrast, we failed to detect any *tri* gene transcripts from the transcriptomic data of *P. bilix*. Curiously, among the four *tri* genes in cryptophytes (i.e. *Py. helgolandii* and *Gu. theta*), the *tri1* transcript was missing in both *Goniomonas* spp. and *R. truncata*, suggesting that the *tri1* gene likely encodes a protein that is unique to cryptophycean ejectisomes. Alternatively, we may have overlooked the *tri1* gene sequences in the transcriptomic data from *Goniomonas* spp. and/or *R. truncata*, in case of the goniomonad and/or kathablepharid homologues being too diverged from the cryptophyte homologues. To understand the conservation, diversity, and evolution of cryptist ejectisomes, the data regarding protein components in both goniomonad and kathablepharid ejectisomes are indispensable.

The chromalveolate hypothesis assumes that cryptophytes, haptophytes, stramenopiles, and alveolates derived from a common ancestor bearing a red alga-derived plastid²⁹. As cryptophytes are nested within phagotrophic lineages in the Cryptista clade, this hypothesis demands the ancestral cryptist cell to operate both phagocytosis and photosynthesis (i.e., mixotrophy), followed by changes in lifestyle after the divergence of cryptists—specifically, cryptophytes and other cryptist members would have abandoned phagocytosis and photosynthesis, respectively (Fig. 3b, left). Alternatively, it is also possible that the ancestral cryptist cell was a non-photosynthetic predator, and photosynthesis was established after the split of cryptophytes and goniomonads (Fig. 3b, right).

Both morphological/ultrastructural and molecular data from *P. bilix* are useful to understand character evolution in Cryptista.

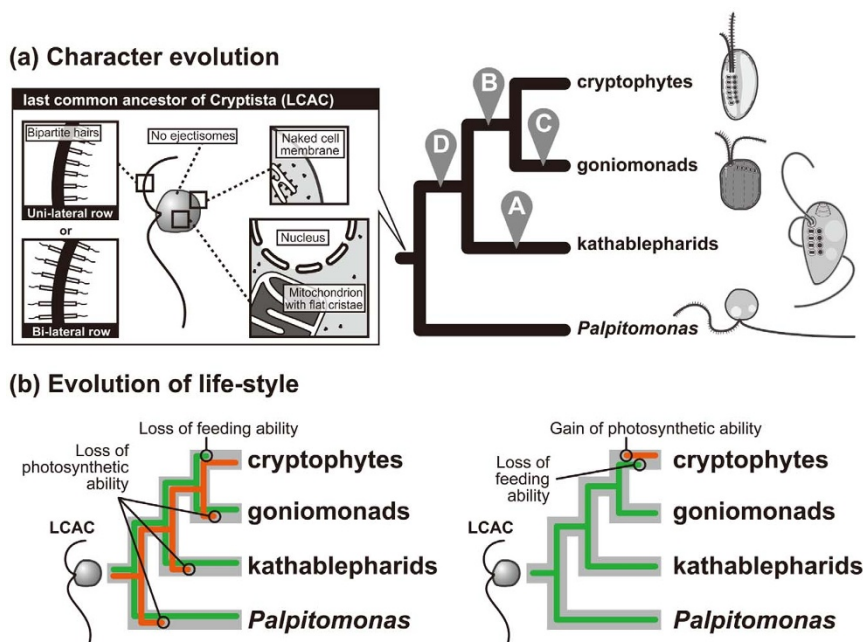


Figure 3 | Character evolution in the Cryptista. (a). The phylogenetic relationship among cryptophytes, goniomonads, kathablepharids, and *Palpitomonas bilix*, based on the 157-gene phylogeny (see Fig. 1). The putative morphology and ultrastructural characteristics of the last common ancestor of the Cryptista (LCAC) are schematically illustrated. A, Acquisition of the sheath and the conoid-shaped feeding apparatus, loss of bipartite flagellar hairs, and ‘flat-to-tubular’ transformation of the mitochondrial cristae; B, Acquisition of the periplast; C, Acquisition of spines and simplification of flagellar hairs; D, Acquisition of ejectisomes. (b). Alternative scenarios of the evolution of lifestyle in Cryptista. Green and orange lines represent phagotrophic and photosynthetic capacities, respectively. left, LCAC employed both phagocytosis and photosynthesis, as anticipated from the chromalveolata hypothesis²⁹; right, LCAC was a non-photosynthetic predator.

Nevertheless, we need to re-examine the phylogenetic affiliation of Picozoa (see the above discussion) and to survey novel microbial eukaryotes in natural environments, since the true diversity of Cryptista has yet to be uncovered. For instance, environmental PCR surveys have detected two uncultured cryptomonad lineages, CRY-1 and CRY-3^{30,31}, and the morphological and molecular data from CRY-1 and CRY-3 are essential to fill the gaps between cryptophytes and goniomonads. We also anticipate that novel cryptist members, which represent lineages branching earlier than *P. bilix*, remain undetected in nature. Such novel cryptists, if they exist, are significant to understand the early evolution of Cryptista, and help resolving the position of Cryptista in the tree of eukaryotes.

Methods

Cultures, RNA extraction and sequencing. *Palpitomonas bilix* NIES-2562 was maintained in the laboratory at the University of Tsukuba. *Goniomonas* sp. ATCC PRA-68 was purchased from the American Type Culture Collection (ATCC). *Palpitomonas bilix* and *Goniomonas* sp. were grown in ESM and URO-YT media³², respectively, at 20°C. Approximately 4.19×10^8 cells of *P. bilix* and 1.31×10^8 cells of *Goniomonas* sp. were harvested from approximately 15 L of 1-week-old cultures. Total RNA was extracted from the harvested cells using Trizol (Life Technologies, Carlsland, CA, USA) by following the manufacturer’s protocol. This yielded 0.734 and 0.777 mg of total RNA of *P. bilix* and *Goniomonas* sp., respectively. cDNA library construction and 454 pyro-sequencing by the GS FLX system (454 Sequencing, Roche, Nutley, NJ, USA) were performed at Dragon Genomics Center (TAKARA Bio, Mie, Japan). 104,136 and 132,161 single-path reads from the *P. bilix* and *Goniomonas* sp. libraries were assembled into 8,586 and 8,394 contigs, respectively, by the MIRA assembly program version 3.2³³ with accurate option. The raw sequence data were deposited to GenBank as DRR013022 (*P. bilix*) and DRR013023 (*Goniomonas* sp.). The contig sequences are available from the corresponding author upon request.

Phylogenomic analysis. The contig (nucleotide) sequences of *P. bilix* and *Goniomonas* sp. were conceptually translated into amino acid sequences by ExpASY translation tool website (<http://web.expasy.org/translate>), and then added and aligned to the single-protein datasets analyzed in Kamikawa et al.¹⁷ manually. We also added the sequence data of *R. truncata*, *Collodictyon triciliatum*, *Galdieria sulphuraria*, and *Cyanophora paradoxa*. Ambiguously aligned positions were excluded from individual alignments manually. Each of the single-protein datasets were subjected to maximum-likelihood (ML) phylogenetic analysis with the LG

model³⁴ incorporating empirical amino acid frequencies and among-site rate variation approximated by a discrete gamma distribution with four categories (LG + Γ + F model), in which heuristic tree searches were performed based on 10 randomized maximum-parsimony (MP) starting trees. One hundred bootstrap replicates were generated from each dataset, and then subjected to ML bootstrap analysis with the LG + Γ + F model, in which heuristic tree searches were performed from a single MP tree. RAXML ver. 7.6.3³⁵ was used for the ML analyses described above. Occasionally, individual protein datasets failed to recover monophyly of Opisthokonta, Amoebozoa, Alveolata, Stramenopiles, Rhizaria, Rhodophyta, Viridiplantae, Glaucophyta, Haptophyta, Cryptophyta, Jakobida, Euglenozoa, Heterolobosea, Diplomonadida, Parabasalia, and/or Malawimonadida, because of contamination, erroneous incorporation of paralogues or lateral gene transfers. These cases were detected by searching for splits in individual protein trees that were supported ML bootstrap values $\geq 70\%$ and that conflicted with the well-accepted taxonomic groups listed above (data not shown). We manually identified the sequences that were responsible for these conflicts, and excluded them from the phylogenomic analyses described below. The single-gene alignments were then combined into a phylogenomic (157-gene) alignment. The dataset analyzed in the present study was composed of sequence data from multi-cellular eukaryotes and microbial eukaryotes maintained in the laboratory (see Results for the reason for including no uncultivated organism in the phylogenomic alignment). After preliminary analyses, several rapidly evolving (long-branched) taxa (e.g., *Trichomonas* and *Giardia*) were excluded. The final alignment includes 64 taxa with 41,372 amino acid positions. The detailed gap information of each single-gene alignment is supplied in Table S1. The single-gene and 157-gene alignments are available from https://sites.google.com/site/ryomakamikawa/Home/dataset/palpitomonas_2013.

The 157-gene alignment was phylogenetically analyzed by the ML and Bayesian methods using RAXML ver. 7.6.3 and PHYLOBAYES MPI ver. 1.3b³⁶, respectively. For ML and ML bootstrap analyses, we applied the LG4X model, which allows amino acid equilibrium frequencies and their exchangeabilities to vary across four categories under a distribution-free scheme for site rates³⁷. We evaluated Akaike Information Criterion scores for all of the amino acid substitution models implemented in RAXML, and the LG4X model was selected as the most appropriate one to analyze the 157-gene alignment (Table S2). The ML tree was heuristically searched from 10 randomized MP starting trees. In ML bootstrap analyses (100 replicates), heuristic tree search was performed from a single MP tree per replicate. We also subjected the 157-gene alignment to Bayesian analysis with the CAT-Poisson model incorporating among-site rate variation approximated by a discrete gamma distribution. Two Markov chain Monte Carlo (MCMC) runs were run for 10,000 generations, sampling log-likelihoods every 10 trees. Bayesian posterior probabilities were calculated after discarding the first 25% of the trees stored during MCMC as ‘burn-in’ (‘maxdiff’ value = 0.24).



Database surveys of *tri* genes. The putative homologues of *tri1*, *tri2*, *tri3-1* and *tri3-2*, which encode the proteins comprising the ejectisomes in the cryptophyte *Pyrenomonas helgolandii*²¹, were searched in the transcriptomic data from *P. bilix*, *Goniomonas* sp., and *R. truncata*, as well as in the genome data of the cryptophyte *Gu. theta*. The nucleotide sequences of *tri1*, *tri2*, *tri3-1* and *tri3-2* of *P. helgolandii* were used as the queries for tblastx surveys with *E*-value cut-off 10^{-10}. The deduced amino acid sequences of *Tri* proteins were manually aligned. *tri1* or *tri1*-like sequences were further surveyed in the transcriptomic data of *Goniomonas* sp. and *R. truncata* by HMMER²². The HMM profile was generated from cryptophyte *Tri1* amino acid sequences (GenBank accession numbers AFH35045.1, XP_005829861.1, XP_005830134.1, XP_005841702.1, and XP_005824080.1).

- López-García, P., Philippe, H., Gail, F. & Moreira, D. Autochthonous eukaryotic diversity in hydrothermal sediment and experimental microcolonizers at the Mid-Atlantic Ridge. *Proc. Natl. Acad. Sci. U S A.* **100**, 697–702 (2003).
- Massana, R., Guillou, L., Díez, B. & Pedrós-Alió, C. Unveiling the organisms behind novel eukaryotic ribosomal DNA sequences from the ocean. *Appl. Environ. Microbiol.* **68**, 4554–4558 (2002).
- Moore, R. B. *et al.* A photosynthetic alveolate closely related to apicomplexan parasites. *Nature*. **451**, 959–963 (2008).
- Yabuki, A., Ishida, K. & Cavalier-Smith, T. *Rigifila ramosa* n. gen., n. sp. Filose amoeba with a distinct pellicle, is related to *Micronuclearia*. *Protist*. **164**, 75–88 (2013).
- Seenivasan, R., Sausen, N., Medlin, L. K. & Melkonian, M. *Picomonas judraskeda* gen. et sp. nov.: the first identified member of the Picozoa phylum nov., a widespread group of picoeukaryotes, formerly known as ‘picobiliphytes’. *PLoS ONE*. **8**, e59565 (2013).
- Not, F. *et al.* Picobiliphytes: a marine picoplanktonic algal group with unknown affinities to other eukaryotes. *Science*. **315**, 253–255 (2007).
- Yabuki, A., Inagaki, Y. & Ishida, K. *Palpitomonas bilix* gen. et sp. nov.: A novel deep-branching heterotroph possibly related to Archaeplastida or Hacrobia. *Protist*. **161**, 523–538 (2010).
- Keeling, P. J. The endosymbiotic origin, diversification and fate of plastids. *Phil. Trans. R. Soc. B.* **365**, 729–748 (2010).
- Okamoto, N., Chantangsri, C., Horák, A., Leander, B. S. & Keeling, P. J. Molecular phylogeny and description of the novel katablepharid *Roombia truncata* gen. et sp. nov., and establishment of the Hacrobia taxon nov. *PLoS ONE*. **4**, e7080 (2009).
- Cavalier-Smith, T. Symbiogenesis: Mechanisms, evolutionary consequences, and systematic implications. *Annu. Rev. Ecol. Syst.* **44**, 145–172 (2013).
- Rice, D. W. & Palmer, J. D. An exceptional horizontal gene transfer in plastids: gene replacement by a distant bacterial paralog and evidence that haptophyte and cryptophyte plastids are sisters. *BMC Biology*. **4**, 31 (2006).
- Ishida, K. *et al.* Comprehensive SSU rRNA Phylogeny of Eukaryota. *Endocyt. Cell Res.* **20**, 81–88 (2010).
- Archibald, J. M. The puzzle of plastid evolution. *Curr. Biol.* **19**, R81–R88 (2009).
- Cavalier-Smith, T. Kingdoms Protozoa and Chromista and the eozoan root of the eukaryotic tree. *Biol. Lett.* **6**, 342–345 (2009).
- Burki, F., Okamoto, N., Pombert, J. F. & Keeling, P. J. The evolutionary history of haptophytes and cryptophytes: phylogenomic evidence for separate origins. *Proc. Biol. Sci.* **B. 279**, 2246–2254 (2012).
- Burki, F. *et al.* Phylogenomic reshuffles the eukaryotic supergroups. *PLoS ONE*. **2**, e790 (2007).
- Kamikawa, R. *et al.* Gene content evolution in discobid mitochondria deduced from the phylogenetic position and complete mitochondrial genome of *Tsukubamonas globosa*. *Genome Biol. Evol.* **6**, 306–315 (2014).
- Zhao, S. *et al.* *Collocticyon* - an ancient lineage in the tree of eukaryotes. *Mol. Biol. Evol.* **29**, 1557–1568 (2012).
- Yoon, H. S. *et al.* Single-cell genomics reveals organismal interactions in uncultivated marine protists. *Science*. **332**, 714–717 (2011).
- Kugrens, P., Lee, R. E. & Corliss, J. O. Ultrastructure, biogenesis, and functions of extrusive organelles in selected non-ciliate protists. *Protoplasma*. **181**, 164–190 (1994).
- Yamagishi, T., Kai, A. & Kawai, H. Trichocyst ribbons of a cryptomonad are constituted of homologs of R-body proteins produced by the intracellular parasitic bacterium of *Paramecium*. *J. Mol. Evol.* **74**, 147–157 (2012).
- Eddy, S. R. Accelerated profile HMM searches. *PLoS Computat. Biol.* **7**, e1002195 (2011).
- Cavalier-Smith, T. & Chao, E. E. *Oxnerella micra* sp. n. (Oxnerellidae fam. n.), a tiny naked centrohelid, and the diversity and evolution of heliozoa. *Protist*. **163**, 574–601 (2012).
- Kugrens, P. & Lee, R. E. Organization of cryptomonads. *The Biology of Free-living Heterotrophic Flagellates*. Patterson, D. J. & Larsen, J. (eds.). 219–233 (Clarendon press, Oxford, 1991).

- Mignot, J. P. Étude ultrastructurale de (*Cyathomonas truncata*) from (flagellé Cryptomonadine). *J. Microsc. (Paris)*. **4**, 239–252 (1965).
- Clay, B. & Kugrens, P. Systematics of the enigmatic katablepharids, including EM characterization of the type species, *Katablepharis phoenikoston*, and new observations on *K. remigera* comb. nov. *Protist*. **150**, 43–59 (1999).
- Lee, R. E. & Kugrens, P. *Katablepharis ovalis*, a colorless flagellate with interesting cytological characteristic. *J. Phycol.* **27**, 505–513 (1991).
- Kugrens, P., Lee, R. E. & Andersen, R. A. Ultrastructural variations in cryptomonad flagella. *J. Phycol.* **23**, 511–518 (1987).
- Cavalier-Smith, T. Principles of protein and lipid targeting in secondary symbiogenesis: Euglenoid, dinoflagellate, and sporozoan plastid origins and the eukaryote family tree. *J. Eukaryot. Microbiol.* **46**, 347–366 (1999).
- Shalchian-Tabrizi, K. *et al.* Diversification of unicellular eukaryotes: cryptomonad colonizations of marine and fresh waters inferred from revised 18S rRNA phylogeny. *Environ. Microbiol.* **10**, 2635–2644 (2008).
- Kim, E. & Archibald, J. M. Ultrastructure and molecular phylogeny of the cryptomonad *Goniomonas avonlea* sp. nov. *Protist*. **164**, 160–182 (2013).
- Kasai, F., Kawachi, M., Erata, M., Mori, F., Yumoto, K., Sato, M. & Ishimoto, M. NIES-collection list of strains, 8th edition. *Jap. J. Phycol. (Sôrii)* **57** (Suppl.), 1–350 (2004).
- Chevreur, B. *et al.* Using the miraEST assembler for reliable and automated mRNA transcript assembly and SNP detection in sequenced ESTs. *Genome Res.* **14**, 1147–1159 (2004).
- Le, S. Q. & Gascuel, O. An improved general amino acid replacement matrix. *Mol. Biol. Evol.* **25**, 1307–1320 (2008).
- Stamatakis, A. RAXML-VI-HPC: Maximum likelihood based phylogenetic analyses with thousands of taxa and mixed models. *Bioinformatics*. **22**, 2688–2690 (2006).
- Lartillot, N., Rodrigue, N., Stubbs, D. & Richer, J. PhyloBayes MPI: Phylogenetic reconstruction with infinite mixtures of profiles in a parallel environment. *Syst. Biol.* **62**, 611–615 (2013).
- Le, S. Q., Dang, C. C. & Gascuel, O. Modeling protein evolution with several amino acid replacement matrices depending on site rates. *Mol. Biol. Evol.* **29**, 2921–2936 (2012).

Acknowledgments

We are grateful to Dr. Andrew J. Roger (Dalhousie University, Canada) for his technical helps and suggestions. We also thank Dr. Aaron Heiss (University of Tsukuba, Japan) for critical comments and English-language corrections. A.Y., R.K., and S.A. I. were supported by Research Fellowships from the Japanese Society for the Promotion of Science (JSPS) for Young Scientists (Nos. 201242 and 236484 for A.Y., 210528 for R.K., and 24007 for S.A.I.). M.K. was supported by a Discovery grant (227085-2011) from the Natural Sciences and Engineering Research Council of Canada awarded to Andrew J. Roger. This work was supported by grants from the JSPS awarded to Y.I. (Nos. 21370031, 22657025, and 23117006). Maximum-likelihood phylogenetic analyses conducted in the present work have been carried out under the “Interdisciplinary Computational Science Program” in Center for Computational Sciences, University of Tsukuba.

Author contributions

A.Y., R.K., K.I. and Y.I. designed and performed the experiments, analyzed the data. M.K., S.A.I., E.K., A.S.T. and K.K. gave technical support and additional data. All authors discussed results and implications. A.Y. and Y.I. wrote the manuscript. All authors commented on the manuscript.

Additional information

Supplementary information accompanies this paper at <http://www.nature.com/scientificreports>

Competing financial interests: The authors declare no competing financial interests.

How to cite this article: Yabuki, A. *et al.* *Palpitomonas bilix* represents a basal cryptist lineage: insight into the character evolution in Cryptista. *Sci. Rep.* **4**, 4641; DOI:10.1038/srep04641 (2014).



This work is licensed under a Creative Commons Attribution-NonCommercial-NoDerivs 3.0 Unported License. The images in this article are included in the article’s Creative Commons license, unless indicated otherwise in the image credit; if the image is not included under the Creative Commons license, users will need to obtain permission from the license holder in order to reproduce the image. To view a copy of this license, visit <http://creativecommons.org/licenses/by-nc-nd/3.0/>